Design and advanced characterization of quercetin-loaded nano-liposomes prepared by high-pressure homogenization

Food Chemistry

Nanoliposomes delivering quercetin as senolytic compound: characterization at the nano level and in vitro toxicological effect

--Manuscript Draft--

Manuscript Number:	
Article Type:	Research Article (max 7,500 words)
Keywords:	senolytics; liposomes; high pressure homogenization; analytical ultracentrifugation; nano delivery system; elderly
Corresponding Author:	Sofia Melchior ITALY
First Author:	Sofia Melchior
Order of Authors:	Sofia Melchior
	Marta Codrich
	Andrea Gorassini
	Dora Mehn
	Jessica Ponti
	Giancarlo Verardo
	Gianluca Tell
	Luigi Calzolai
	Sonia Calligaris
Abstract:	Quercetin selected as senolytic compound was included into liposomes produced by high pressure homogenization. Particle size, surface charge, and morphology of structures were comprehensively characterized at the nano level by applying traditional and innovative methodologies (i.e. analytical ultracentrifugation, multi-detector asymmetrical-flow field flow fractionation, transmission electron microscopy). The in vitro toxicological effect of loaded liposomes against HCT116 colon cancer cell line was also evaluated. The majority of structures were characterized by oblong shape and dimensions around 30 nm that may have a pivotal role in the physiological outcome. Moreover, the HCT116 cell line was significantly more sensitive to loaded liposomes compared to free quercetin. These results open new frontiers in the design of delivery systems for senolytic components to be included in foods tailored for the ageing population.
Suggested Reviewers:	Antonio Augusto Vicente University of Minho Centre of Biological Engineering avicente@deb.uminho.pt Research area: food nanostructure, nutritional functionalities, structural characterization
	Like Mao China Agricultural University, College of Food Science and Nutritional Engineering likemao@cau.edu.cn Research area: delivery systems, liposomes, structure characterization
	Adilia Lemos Abertay University Division of Engineering and Food Science a.lemos@abertay.ac.uk Research area: Food chemistry and bioactive compounds

Dear Editor,

We would like to submit the manuscript entitled "*Nanoliposomes delivering quercetin as senolytic compound: characterization at the nano level and in vitro toxicological effect"* by Sofia Melchior, Marta Codrich, Andrea Gorassini, Dora Mehn, Jessica Ponti, Giancarlo Verardo, Gianluca Tell, Luigi Calzolai, and Sonia Calligaris for publication in *Food Chemistry*.

This study is part of a wider research activity dealing with the promotion of the active and healthy ageing of the population, which is a worldwide priority for the scientific community and policymakers. Senolytic therapy is an emerging strategy to promote senescent cell replacement and represents a promising perspective also for designing novel anticancer strategies in combination with current chemotherapy regimens. Different compounds, such as polyphenols, have demonstrated senolytic activity due to their ability to regulate cell senescence, ageing, and longevity. However, the inclusion of these compounds into foods is challenging due to their low water solubility, bioavailability, and stability. The design of carriers for senolytics represents a promising strategy to deliver them in foods up to the target human site. The in-depth characterization of these nanosized structures and their interaction with human cells is pivotal to assess and tailor their functionalities.

The aim of this research was to design and characterize nanoliposomes for the delivery of the senolytic quercetin. To this purpose, high pressure homogenization was used to structure liposomes whose size and shape were investigated by innovative techniques commonly used in nanomedicine field. Senolytic action was investigated by analysing *in vitro* toxicological effect of loaded liposomes against colon cancer cell line. Results confirmed the efficacy of the strategy applied opening new opportunities in food and drug sectors for the promotion of the active and healthy ageing of the population.

Best regards,

27 February 2023

Sofia Melchior

Luigi Calzolai

Highlights

- Liposomes loading senolytic quercetin were produced by high pressure homogenization
- The best-performing treatment for liposome production was 150 MPa for 1 pass
- Liposomes had oblong shape, size around 30 nm and encapsulation efficiency of 42%
- Loaded liposomes exhibited higher senolytic action compared to free quercetin

Nanoliposomes delivering quercetin as senolytic compound: characterization at the nano level and *in vitro* toxicological effect

Sofia Melchior [a*], Marta Codrich [b], Andrea Gorassini [c], Dora Mehn [d], Jessica Ponti [d], Giancarlo Verardo [a], Gianluca Tell [b], Luigi Calzolai [d*], Sonia Calligaris [a]

[a] Department of Agricultural, Food, Environmental and Animal Sciences, University of Udine, Udine, Italy

[b] Department of Medical and Biological Sciences, University of Udine, Udine, Italy

[c] Department of Humanities and Cultural Heritage, University of Udine, Udine, Italy

[d] European Commission, Joint Research Centre (JRC), Ispra, Italy

* Corresponding authors: sofia.melchior@uniud.it, luigi.calzolai@ec.europa.eu

Abstract

Quercetin selected as senolytic compound was included into liposomes produced by high pressure homogenization. Particle size, surface charge, and morphology of structures were comprehensively characterized at the nano level by applying traditional and innovative methodologies (i.e. analytical ultracentrifugation, multi-detector asymmetrical-flow field flow fractionation, transmission electron microscopy). The *in vitro* toxicological effect of loaded liposomes against HCT116 colon cancer cell line was also evaluated. The majority of structures were characterized by oblong shape and dimensions around 30 nm that may have a pivotal role in the physiological outcome. Moreover, the HCT116 cell line was significantly more sensitive to loaded liposomes compared to free quercetin. These results open new frontiers in the design of delivery systems for senolytic components to be included in foods tailored for the ageing population.

Keywords: senolytics, liposomes, high pressure homogenization, analytical ultracentrifugation, nano delivery system, elderly

1 Introduction

Cell senescence is a permanent and irreversible cell cycle arrest that is accompanied by changes in cell morphology and physiology (Kirkland & Tchkonia, 2017). This phenomenon is characterized by different and opposite effects. It is a matter of fact that senescence evolved as a beneficial response to damage promoting wound healing, limiting fibrosis, fighting against cancer, and helping embryonic development. However, the excessive accumulation of senescent cells favours ageing-related diseases as well as other changes associated with ageing and is also an emerging hallmark of cancer chemoresistance (Mária & Ingrid, 2017). Therefore, the design of strategies to selectively reduce senescent cells and improve healthy condition of ageing population is of the utmost importance.

Senolytic therapy is an emerging strategy to promote senescent cell replacement, currently in clinical trial for age-related diseases such as sarcopenia, and represents a promising perspective also for designing novel anticancer strategies in combination with current chemotherapy regimens (Chaib, Tchkonia, & Kirkland, 2022). Different compounds have been indicated to exert senolytic activity. Among them, some plant-derived compounds, such as polyphenols, are indicated as promising in regulating cell senescence, ageing, and longevity. As well known, polyphenols represent a large class of natural compounds present in many fruits and vegetables as well as derived products. Typical examples of polyphenols with senolytic activity are quercetin, catechins, cyanidin, curcumin, and resveratrol (Gurău et al., 2018). In particular, quercetin exerts two complementary actions: on one hand, it can promote the death of ageing cells, while on the other hand, it can delay cell senescence and/or promote clearance of senescent cells in healthy tissues (Gurău et al., 2018; Hwang, Tran, Rebuffatti, Li, & Knowlton, 2018).

Unfortunately, the simply ingestion of quercetin is not sufficient to guarantee its benefits *in vivo* mainly due to its low bioavailability, *i.e.* the fraction of an ingested compound that eventually ends up in the systemic circulation reaching the site of action in an active form (Chen, Zou, Liu, & McClements, 2016). This is attributed to the physical properties of quercetin, *i.e.* crystallinity and

scarce solubility in water (Aditya et al., 2014; Chen et al., 2016; Toniazzo, Peres, Ramos, & Pinho, 2017), as well as to its chemical instability being easily degradable and oxidable under moderate alkaline conditions and/or under heat exposure (Aditya et al., 2014).

These issues may be overcome by designing proper nanostructured delivery systems, such as: liposomes, emulsions, solid lipid nanoparticles, and lipid nanocarriers in order to encapsulate, protect, and release quercetin at the target site of action (Aditya et al., 2014; Toniazzo et al., 2017). Among them, liposomes – defined as self-assembled vesicles ranging from 10 nm to several micrometres with a phospholipid bilayer structure that separates them from the surrounding aqueous environment have received particular attention (Liu et al., 2020). Several studies have demonstrated the aptitude of liposomes as delivery system for quercetin by guaranteeing both its high stability during storage and bioavailability, while ensuring high encapsulation efficiency (Hao et al., 2017; Toniazzo et al., 2017). The effectiveness of liposomes as delivery systems greatly depends on their dimensions (Haddadzadegan, Dorkoosh, & Bernkop-Schnürch, 2022). It is well known that the particle size of the designed structures is a pivotal factor for their application in food as well as in pharmaceutical products (McClements, 2018). Moreover, considering the physiological behaviour, particle dimensions impact body adsorption, biodistribution in the bloodstream, and excretion behaviour (Gioria et al., 2018). The smaller the particle size, the greater is the surface area exposed to lipase digestion, which may influence the release of the encapsulated bioactive compound and thus its bioaccessibility (Álvarez et al., 2022). Additionally, the smaller the size, the higher is the diffusion coefficient in intestinal mucus especially when the nanocarrier has dimensions below 100-200 nm that is the mesh size of the mucus microstructure (Haddadzadegan et al., 2022). With this regard, attention should be paid to the methodology applied to study the morphology and dimensions of liposomes at the nano-level. No single technique can provide reliable information itself about particle size and distribution, but a combination of instruments, based on different operating principles, is likely to be required for a robust nanometric assessment (Calzolai, Gilliland, & Rossi, 2012). In particular, analytical methods, applied in other fields (*e.g.* medical, environmental), may be adapted

to nanostructures intended for food applications. In particular, the usage of nanoparticle tracking analysis, asymmetrical-flow field flow fractionation, or analytical ultracentrifugation together with microscope analysis (*i.e.* transmission electron microscopy) may represent a promising strategy for deep characterization (Gioria et al., 2018).

To obtain liposomes, different mechanical (*i.e.* supercritical carbon dioxide, ultrasounds, and high-pressure homogenization) and non-mechanical (*i.e.* reverse-phase evaporation and ethanol injection) interventions can be exploited (Ibišević, Smajlović, & Arsić, 2019; Wagner & Vorauer-Uhl, 2011). Among these, high-pressure homogenization (HPH) guarantees high reproducibility without solvent utilization and allows to generate liposomes with dimensions lower than 100 nm. Moreover, homogenization process could be easily scaled-up since dedicated equipment are already commercially available (Ibišević et al., 2019; Wagner & Vorauer-Uhl, 2011). Besides the process, the choice of the amphiphilic molecule forming liposomes is crucial. Among all, soy lecithin has received great attention due to its abundance as natural source, relatively low production costs compatibility with cell membranes (Quach et al., 2022)

Based on these considerations, the aim of the present study was to design nano-liposomes for the delivery of the senolytic quercetin. To this purpose, in the first part of the study, HPH at different processing conditions in terms of homogenization pressure and number of steps was applied to structure lecithin-based liposomes. The resulting systems were then characterized for their size, ζ-potential, and encapsulation efficiency. The best performing process conditions were then used to prepare quercetin loaded nano-liposomes, whose nanostructure was further characterized by applying techniques commonly used in nanomedicine, such as multi-detector asymmetrical-flow field flow fractionation (AF4) and analytical ultracentrifugation (AUC). Finally, the metabolic effect of quercetin-loaded liposomes against colon cancer cells was evaluated.

2 Materials and methods

2.1 Materials

Pure soy lecithin was purchased from Carlo Erba Reagenti SpA (Rodano, Milan, Italy); potassium phosphate (K_2HPO_4), quercetin (≥95%), kaempferol (≥ 97%; HPLC-DAD Internal Standard; IS), methanol (MeOH) and formic acid for HPLC-MS were purchased from Sigma-Aldrich. HCT-116 $p53^{+/+}$ cells were provided by ATCC (Manassas, USA). Dulbecco's modified Eagle's medium, fetal bovine serum, GlutaMAX, penicillin, and streptomycin were provided by EuroClone (Milan, Italy) Milli-Q grade water was produced by the Elgastat UHQ-PS system (ELGA, High Wycombe Bucks, UK).

2.2 Liposome preparation

Soy lecithin (10 g/L) added or not with quercetin (0.3 g/L) was dispersed in water and stirred for 1 h at room temperature. The dispersion was then pre-homogenized with a high-speed homogenizator (Ultra-Turrax Homogenizer, IKA, Germany) for 5 minutes at 14,000 rpm. Then, the sample was homogenized using a continuous lab-scale high-pressure homogenizer (Panda Plus 2000; GEA Niro Soavi, Parma, Italy) characterized by two Re + type tungsten carbide homogenization valves and flow rate of 10 L/h. The treatment was conducted at pressures of 50, 100, and 150 MPa for 1 pass and at 150 MPa for 3 passes. A sample not subject to HPH treatment was used as control (No HPH). To remove unincorporated material, after HPH, samples were centrifuged (Beckman Coulter, AvantiTM centrifuge, J-25, USA) for 10 minutes at 10,000 ×*g* and the supernatant containing liposomes was collected for further analysis, while the precipitate were discarded. Samples were prepared with and without quercetin and stored at 4 °C until further analysis.

2.3 Analytical determinations

2.3.1 Turbidity measurement

Turbidity was measured at 660 nm using a UV-Vis spectrophotometer (UV-2501 PC, Shimadzu, Kyoto, Japan) at 25 °C with a 1 cm path-length cuvette.

2.3.2 Particle size distribution and ζ-potential

Particle size distribution in batch mode was measured by dynamic light scattering (DLS, Zetasizer NanoZS, Malvern Instruments, Worcestershire, UK). Samples were diluted 1:100 (v/v) with MilliQ water and placed in a cuvette where the scattered laser light (at 173° angle) was analysed.

For ζ-potential measurements, samples were placed in a disposable folded capillary cell equipped with two electrodes to assess particle electrophoretic mobility.

2.3.3 Encapsulation efficiency by HPLC-ESI-MS-DAD

Encapsulation efficiency (EE, %) was measured by HPLC-ESI-MS-DAD. Samples were diluted 1:20 (v/v) with methanol to permit the quercetin release from the liposomes.

Each sample (100 μL) was spiked with 100 μL of the IS solution (kaempferol, 9.7 μg/mL in MeOH) and diluted in 1 mL of MeOH/H_2O 70:30 (v/v) with 0.4% of formic acid. The sample was transferred in an autosampler vial for the HPLC-ESI-MS-DAD analysis.

Chromatographic analysis was performed with a UHPLC Ultimate 3000 (Thermo Scientific, San Jose, CA, USA) equipped with a column oven and a thermostated autosampler. The chromatographic separation was performed with a column InfinityLab Poroshell 120 EC-C18 (4.6 × 150 mm, 2.7 μm; (Agilent Technology, Milan, Italy), thermostated at 30 °C. Elution was carried out at a flow rate of 0.3 mL/min, using as mobile phase a mixture of 0.2% formic acid in methanol (A) and 0.2% formic acid in water (B) with the following gradient: 0-13 min 70% A, 15 min 100% A, 26 min 100% A, 28 min 70% A, 35 min 70% A. The injection volume was 20 μL. The HPLC system was coupled with a Ultimate 3000 RS diode array detector (DAD; Thermo Scientific, San Jose, CA, USA) and a Finnigan

158 LXQ linear ion trap mass spectrometer with an electrospray ionization source (ESI-MS; Thermo
159 Scientific, San Jose, CA, USA), in parallel by splitting the mobile phase 1:1. The acquisition was
160 carried out in full scan (*m/z* 50-1500) and in full scan MS^2 (*m/z* 50-600) selecting the precursor ion
161 $[M - H]^-$ at *m/z* 301.1 for quercetin and at *m/z* 285.2 for kaempferol (IS). The quantitative analysis
162 was carried out using a diode array detector controlled by Chromeleon software (version 6.80).
163 Spectral data from all peaks were accumulated in the range of 200-400 nm and chromatograms were
164 recorded at 372 nm for both quercetin and kaempferol (IS).
165 A stock solution of quercetin in MeOH/H_2O 70:30 (v/v) with 0.4% of formic acid was serially diluted
166 with the same solvent, with a constant concentration of kaempferol (0.97 μg/mL), to prepare 6-point
167 calibration curve in the range 0.1-3.0 μg/mL. The R^2 coefficient for the calibration curve was > 0.999.
168 EE (%) was calculated following Eq. 1:
169

170 $$EE\ (\%) = \frac{encapsulated\ quercetin\ (\frac{mg}{mL})}{quercetin\ in\ the\ initial\ dispersion\ (\frac{mg}{mL})}\ x\ 100 \qquad \text{Eq. 1}$$

171

172 *2.3.4 Analytical ultracentrifugation (AUC)*

173 AUC analysis was performed using a Beckman Coulter ProteomeLabTM XL-I analytical
174 ultracentrifuge with an 8-hole rotor, collecting interference and absorbance signals simultaneously in
175 the same run. Samples were diluted with water and measurements were conducted at 20 °C at a
176 rotation speed up to 30,000 rpm. Absorbance signals were collected at 250 and 370 nm. The ls-g*(s)
177 distribution model of the SEDFIT software was applied to fit experimental data to calculate
178 sedimentation coefficient distributions. The latter were transformed to hydrodynamic diameter (Dh)
179 using the "transform s distribution to r distribution" option of SEDFIT. Particle viscosity and density
180 were calculated in accordance with the ISO standard n. 18747-2 (ISO, 2019). Samples were diluted
181 in sucrose solutions (5% w/v) and reference cell of the AUC centrepiece was loaded with sucrose
182 solution of the same density.

2.3.5 Multi-detector asymmetrical-flow field flow fractionation (MD-AF4)

The analysis was performed with AF2000 Multiflow FFF (Postnova Analytics GmbH, Landsberg, Germany) equipped with isocratic pumps (Postnova PN1130), degasser (Postnova PN7520), and a manual injector with a 50 µL loop. The system was equipped with three online detectors: multi-angle laser scattering (MALS, Wyatt DAWN HELEOS II MALS detector (λ=661 nm) equipped with 18 detectors at angles from 12.8° to 157.8°; UV-VIS detector (Postnova 3212) set at 250 nm; and DLS equipped with flow-mode cell, detecting in backscattering at 173°. The mobile phase, consisting of phosphate buffer 1 mM (pH 8), was pumped into the channel from opposite ends during injection and focusing, and came out through a 10 kDa cellulose membrane (294 mm x 30 mm, Postnova) at the accumulation wall. When focusing is complete the analyte forms a thin line transverse to the direction of channel and detector flow. Subsequently, the analyte was separated into components based on size as a result of opposing forces of particle diffusion and applied cross flow rate perpendicular to channel or detector flow rate (Parot, Caputo, Mehn, Hackley, & Calzolai, 2020). The optimized method consisted of a focus-injection step for 5 min, followed by elution at detector flow of 0.5 mL/min with an exponentially decaying cross flow from 0.6 to 0 mL/min for 60 min. In this experiment, 50 µL aliquots of sample were used. Online UV–Vis absorbance at 250 nm was utilized for the estimation of mass recovery (R%). The latter was obtained by integrating the area under the UV–Vis peak for each sample eluted with and without the applied cross flow and focusing step using Nova FFF4 software (Eq.2).

$$R\ (\%) = \frac{\text{UV–Vis area of fractionated sample}}{\text{UV–Vis area of sample without crossflow or focus}} * 100 \qquad \text{Eq. 2}$$

Although different parameters were considered and modified (cross flow, injection time, sample amount and concentration, mobile phase composition and pH) to optimize the process, the maximum recovery (R%) was below 70% that is the minimum limit required by ISO/TS 21362 (ISO, 2018).

However, the fractogram and the increase of particle size with the exit time indicated that the applied method was satisfactory to achieve the separation of liposomes with different sizes while guaranteeing high reproducibility (Iavicoli et al., 2015).

The geometric diameter (Dg) was computed through the Wyatt ASTRA software by using the Zimm model, typically applied for small particles, and the sphere model obtaining R^2 higher than 0.7 and 0.9, respectively. The hydrodynamic diameter (Dh) was obtained by analysing DLS flow data with the Zetasizer software. The shape factor was calculated as the ratio between Dg and Dh. For each sample, the analysis was performed in triplicate.

2.3.6 Transmission electron microscope (TEM)

Shape and size of liposomes were analysed by direct visualization using Cryo-TEM technique (Burrows and Penn, 2013). Briefly, 4 µL of liposomes stock suspension were applied to 200 mesh copper Lacey Carbon Film grid (Agar Scientific, UK) pre-treated by Leica EM ACE200 glow discharge (10mA, 30s; Leica, Italy). Excess material was blotted away by filter paper and sample vitrification was done using Leica EM GP (Leica, Italy) equipment. Sample was immediately analysed by TEM at 120kV (JEOL-JEM 2100, JEOL, Italy) equipped with Gatan cryo transfer holder 626 (Gatan, USA).

2.4 Cell cultures

HCT-116 $p53^{+/+}$ (ATCC) cells were grown in Dulbecco's modified Eagle's medium supplemented with 10% fetal bovine serum, 2 mM GlutaMAX and 100 U/mL penicillin and 10 µg/mL streptomycin.

2.4.1 Cell Metabolic Assay

Cell line viability was measured using the colorimetric method CellTiter 96® AQueous One Solution Proliferation assay (MTS) (Promega, Madison, WI, USA) according to the manufacturer's protocol. In detail, 5000 cells were plated on transparent 96-well plates. The day after, cells were treated with

empty liposomes, quercetin-loaded liposomes, or quercetin alone, and the viability of the cells was measured by recording the absorbance at 490 nm with a plate reader (Enspire PerkinElmer, Waltham, MA, USA).

2.5 Statistical analysis

All determinations were expressed as the mean ± standard deviation (SD) of at least three measurements. Analysis of variance (ANOVA) and t-test were performed by using R v. 4.1.1 for Windows (The R foundation for statistical computing). A Tukey's *post-hoc* test was used to assess differences between means ($p<0.05$).

3 Results and discussion

3.1 Definition of the best processing condition for liposome preparation

The effect of high-pressure homogenization (HPH) conditions (pressure and number of passes) on liposome formation was firstly evaluated. Table 1 shows turbidity, measured at 660 nm, particle size distribution, ζ-potential, and encapsulation efficiency (EE) of liposomes with and without quercetin. The turbidity of liposomes without quercetin decreased as the homogenization pressure increased. However, by increasing the number of passes at 150 MPa further increased the turbidity values. Since turbidity is associated to the size and distribution of particles, particle size distribution was also analysed (Figure S 1). All samples were polydisperse as indicated by PDI values higher than 0.2. The control sample presented the highest Z-average (Z-ave) and PDI above 0.5 indicating very broad size distribution (Figure S 1a). The application of HPH induced the formation of liposomes with less polydisperse distributions that decreased as a function of pressure increase and as a result of increased intensity of shear forces suffered by the sample during the passage through the homogenization valve. Sample prepared at 150 MPa for 1 pass had the lowest PDI (0.282 ± 0.007) and Z-ave of 69.3 ± 0.8 nm. These results were in agreement with previous studies that reported the dependence of particle size reduction on HPH pressure increase (Barnadas-Rodríguez & Sabés, 2001). Although Z-ave was

the lowest, by further increase HPH intensity (150 MPa for 3 passes) PDI of liposomes significantly (p<0.05) increased, indicating the reduction of size homogeneity probably due to aggregation and/or destabilization of particles upon treatment (Ibišević et al., 2019).

Similar results were observed for quercetin-loaded liposomes. Overall, compared with unloaded samples, liposomes with quercetin were characterized by higher turbidity and particle dimensions (Figure S 1) probably because the bioactive compound affected liposome characteristics. This phenomenon was also observed by Toniazzo *et al.* (2017) that reported average particle size of quercetin loaded liposomes higher than that of unloaded ones. Similarly, Gibis, Ruedt, & Weiss (2016) observed the same behaviour when grape-seed polyphenols were incorporated into liposomes. The increase of particle size of loaded structures may be attributed to the location of quercetin closer to the centre of the lipid bilayer. This may adversely affect the colloidal stability of liposomes by reducing the surface exposure of the phosphate head groups leading to the system destabilization (Malekar, Sarode, Bach, & Worthen, 2016).

ζ-potential (Table 1) become more negative by increasing pressure up to 150 MPa, while a slight increase was observed for the sample produced at 150 MPa for 3 passes probably due to system destabilization, as confirmed by previous data. The progressive tendency of ζ-potential to get close to -30 mV indicated that the physical stability of liposomes increased with pressure (Madureira et al., 2015). Interestingly, the effect of treatment was less pronounced in loaded liposomes probably due to the location of quercetin in the middle of lecithin bilayer, which leads to reduced exposure of phosphate groups (Malekar et al., 2016), as previously speculated.

Finally, encapsulation efficiency (EE) (Table 1) ranged from 31% to 42%. These results are in agreement with those by other authors reporting EE between 32% and 50% in the case of liposomes containing black carrot extract produced by HPH (Guldiken, Gibis, Boyacioglu, Capanoglu, & Weiss, 2017). As expected, and in agreement with previous observation, EE increased as a function of pressure increase, achieving the highest value of 42.11 ± 4.08% at 150 MPa, while the lowest one was obtained at 150 MPa for 3 passes. Beside the process conditions, EE results also depend on the

286 solubility of quercetin in the lecithin bilayer (Guldiken et al., 2017). Complete liposome
287 encapsulation may be achieved only if the encapsulated material is soluble in the liposome membrane
288 (Bryła, Lewandowicz, & Juzwa, 2015), as observed considering the delivery of hibiscus (61–72%),
289 elderberry (25%), and grape seed (88%) (Bryła et al., 2015; Gibis et al., 2016; Gibis, Zeeb, & Weiss,
290 2014).
291 Based on the acquired results, liposomes obtained at 150 MPa for 1 pass were selected as the best
292 delivery system due to their smaller particle size, good physical stability, inferred from ζ-potential
293 value, and the highest EE as compared with the other samples.
294
295 *3.2 Nanostructure of liposomes*
296 Quercetin-loaded and unloaded liposomes, produced by applying the best performing condition (150
297 MPa for 1 pass), were in-depth characterized for their size. As previously discussed, DLS in batch
298 mode is not always appropriate to measure the dimensions of nanoparticles (Caputo, Arnould, et al.,
299 2019; Caputo, Clogston, Calzolai, Rösslein, & Prina-Mello, 2019; Gioria et al., 2018; Mehn, Caputo,
300 et al., 2017). Thus, analytical ultracentrifugation (AUC) and asymmetric flow field flow fractionation
301 (AF4) were performed. These techniques have been recently proposed in the nanomedicine field to
302 characterize the size of nanostructures, such as liposomes (Iavicoli et al., 2015; Mehn, Capomaccio,
303 Gioria, Gilliland, & Calzolai, 2020; Mehn, Iavicoli, et al., 2017) and lipid nanoparticles (Caputo,
304 Arnould, et al., 2019).
305 AUC monitors the sedimentation profile of particles in real time and, by the application of a suitable
306 model, allows the calculation of the particle diameter (Planken & Cölfen, 2010) if density of the
307 particles is known. Figure 1 reports the size distribution of liposomes, with or without quercetin,
308 acquired at 250 nm. Free liposomes were characterized by an almost monodisperse distribution with
309 a mean diameter around 30 nm. The same particle family was detected also in loaded samples, but in
310 this case the distribution was broader. An additional peak was observed at 52 nm, while larger
311 particles were depicted to a lesser extent. Loaded samples were also analysed at 370 nm, which is the

312 quercetin peak of absorbance, to evaluate the role of the bioactive molecule on liposome structure.
313 As previously observed, the addition of quercetin probably interfered with liposome formation
314 resulting in structures with higher dimensions (around 65 nm) as compared with the profile acquired
315 at 250 nm and attributable only to lecithin.
316 Overall, AUC results highlighted that the size of the majority of particles was almost three times
317 lower than that measured by DLS in batch mode, which were: 99.3 ± 4.5 nm and 110.6 ± 2.5 nm for
318 unloaded and loaded samples, respectively (Figure S 1d). Such findings also point out the limitations
319 of DLS in batch mode, such as its low resolution in complex media and in presence of multiple
320 populations in similar size ranges, confirming the necessity to apply other techniques, such as AUC,
321 when dealing with particle size characterization in the nano scale (Caputo, Arnould, et al., 2019;
322 Gioria et al., 2018).
323 AUC results were confirmed by data obtained by AF4. The latter is a high-resolution sizing technique
324 based on the introduction of a fractionation step that separates particles based on their size prior to
325 the detection, without affecting their "soft" structure. Moreover, AF4 offers the possibility to combine
326 multiple on-line detectors, overcoming the limitations of traditional batch mode DLS, while ensuring
327 high size measurement (Caputo, Arnould, et al., 2019; Parot et al., 2020). Results acquired by AF4
328 using different detectors (*i.e.* UV-Vis, MALS, and DLS) are reported in Figure 2.
329 Observing the UV-Vis profile of unloaded samples (black line in Figure 2a), two main peaks were
330 detected. The first one (8.6 min) showed the highest intensity, while the second one (between 25 and
331 60 min) was less intense and broader. UV-Vis data were combined with those acquired by MALS
332 detector, in order to obtain information about the geometric diameter (Dg) of liposomes and their
333 abundance. Three main particle families having different dimensions were observed. Two of them
334 (green and red lines in Figure 2a) were detected in correspondence with the highest UV-Vis intensity,
335 indicating that the majority of liposomes belong to these particle families with Dg ranging from 42
336 to 65 nm. The third particle family (violet line in Figure 2a) appeared with the second UV-Vis peak,
337 indicating the presence of liposomes with dimensions higher than 80 nm. Loaded liposomes (Figure

2b) showed the same behaviour but, in this case, the dimensions of the smallest particles were slightly higher (50 - 71 nm).

The availability of the online Dg obtained by MALS, as well as the hydrodynamic diameter (Dh) detected with DLS in flow mode (yellow dots in Figure 2), allows to gain information on the morphology of particles by calculating the shape factor (ρ). It is interesting to note that the majority of liposomes, independently on the addition of quercetin, presented Dg higher than Dh, resulting in ρ >1, which is typical of oblong nanoparticles (*i.e.* nanorods, nanotubes, or nanofibers) (Iavicoli et al., 2015). The applied process conditions (150 MPa for 1 pass) probably favoured the production of spherical uniform liposomes. However, this heterogeneity in particle shape could have a favourable effect not only for the liposome applications in food preparation, but also considering the potential biological fate of incapsulated quercetin (Zhou & McClements, 2022). As observed for drug delivery, rod-shaped particles or non-spherical ones are taken up and transported across the intestinal cells to a greater extent compared to those with spherical shape (Banerjee, Qi, Gogoi, Wong, & Mitragotri, 2016).

Shape and size data were corroborated by direct visualization of liposomes with Cryo-TEM (Figure 3). Micrographs highlighted the presence of structures with heterogeneous dimensions in the same range previously detected by AUC (Figure 1) and AF4 (Figure 2). Moreover, spherical and oblong liposomes were observed, confirming previous speculations. In this regard, it is interesting to note that the treatment applied was able to generate liposomes with different structures (*i.e.* unilamellar, multilamellar, and multivesicular vesicles), that may improve the stability and delay sustained-release of quercetin (Liu et al., 2020).

3.3 Quercetin-loaded liposomes are able to enter colon cancer cells efficiently.

To test the effects of quercetin-loaded liposomes *in vitro*, we took advantages of a colon cancer cell line (HCT-116 $p53^{+/+}$ cells), that is wild-type for TP53 gene expression (Bunz et al., 1998). Experimentally, HCT-116 $p53^{+/+}$ cells were treated with increasing concentrations of quercetin-

loaded liposomes or free quercetin for 48 h. The control cells were treated with unloaded liposomes and the vehicle DMSO, respectively. Then, we evaluated the metabolic activity of viable cells by using the MTS assay (Figure 4). We observed that HCT-116 $p53^{+/+}$ cell line was significantly more sensitive to quercetin-loaded liposomes, at the doses of 50 μM and 100 μM, than free quercetin. We did not find a statistically significant difference between quercetin-loaded liposomes and free quercetin at lower doses, even though a differential effect can be observed. Notably, at 100 μM no differences were detected between loaded and unloaded liposomes. This result could be attributed to soy lecithin that is involved in several metabolic and intracellular process, such as necrosis and apoptosis. Previous studies have also demonstrated that surface active molecules (*i.e.* lecithin, bile salts, phospholipids as well as anionic, cationic, and nonionic surfactants) may reduce the viability of model colon cancer cells through several mechanisms including the disruption of cell membranes, the modification of active transporters, and the competition with the cells for the surface of the cell culture plates, thereby promoting cell detachment (Li, Le Maux, Xiao, & McClements, 2009; Robert, Couëdelo, Vaysse, & Michalski, 2020).

However, treatment with the quercetin-loaded liposomes significantly reduced the metabolic activity of the HCT-116 $p53^{+/+}$ cell line with respect to unloaded liposomes at the doses of 50 μM.

In conclusion, colon cancer cells are significantly more sensitive to quercetin-loaded liposomes compared to free quercetin and unloaded liposomes, meaning that quercetin-loaded liposomes are able to enter the cell in an efficient manner.

4 Conclusions

Lecithin-based liposomes produced by HPH resulted good candidates for the delivering of the senolytic compound quercetin. The process conducted at 150 MPa for 1 pass results the most profitable being able to form liposomes with high encapsulation efficiency and nano-dimensions (around 30 nm), as demonstrated by the use of advances analytical techniques, such as AUC and AF4, scarcely applied in the food sector. The quercetin loaded nano-sized liposomes showed better capacity

to act as senolytic agent in colon cancer cells in comparison free quercetin and unloaded systems. These findings suggest that the delivery of quercetin within liposomes may represent a promising strategy to improve its senolytic activity opening new opportunities in food and drug sectors.

Declaration of Competing Interest

The authors declare that they have no known competing financial interests or personal relationships that could have appeared to influence the work reported in this paper.

Author's contributions

S.M.: Formal analysis, Investigation, Data curation, Methodology, Writing original draft, Visualization, Writing - Review & Editing; M.C.: Formal analysis, Investigation, Data curation, Writing original draft, Visualization, Writing - Review & Editing; A.G.: Formal analysis, Investigation, Data curation, Visualization, Writing original draft, Visualization, Writing - Review & Editing; D.M.: Formal analysis, Investigation, Methodology, Visualization, Writing - Review & Editing, J.P.: Formal analysis, Investigation, Writing - Review & Editing; G.V.: Formal analysis, Investigation, Data curation, Visualization, Writing original draft, Visualization, Writing - Review & Editing; G.T.: Writing original draft, Resources, Visualization, Writing - Review & Editing, Supervision; L.C.: Visualization, Supervision, Resources, Writing - Review & Editing S.C.: Supervision, Visualization, Resources, Writing original draft, Writing - Review & Editing.

Acknowledgements

This work was undertaken as a part of the projects "Personalized Health management of physical, mental and social frailty in the elderly" (Fondazione Friuli, Italy) and Programma specifico n. 72/17 (Codice FP1935148001, CUP G22F19000070009) of Regione Autonoma Friuli Venezia Giulia – FSE - PO 2014/2020.

References

Aditya, N. P., Macedo, A. S., Doktorovova, S., Souto, E. B., Kim, S., Chang, P. S., & Ko, S. (2014). Development and evaluation of lipid nanocarriers for quercetin delivery: A comparative study of solid lipid nanoparticles (SLN), nanostructured lipid carriers (NLC), and lipid nanoemulsions (LNE). *LWT - Food Science and Technology*, *59*, 115–121.

Álvarez, R., Giménez, B., Mackie, A., Torcello-Gómez, A., Quintriqueo, A., Oyarzun-Ampuero, F., & Robert, P. (2022). Influence of the particle size of encapsulated chia oil on the oil release and bioaccessibility during *in vitro* gastrointestinal digestion. *Food and Function*, *13*, 1370–1379.

Banerjee, A., Qi, J., Gogoi, R., Wong, J., & Mitragotri, S. (2016). Role of nanoparticle size, shape and surface chemistry in oral drug delivery. *Journal of Controlled Release*, *238*, 176–185.

Barnadas-Rodríguez, R., & Sabés, M. (2001). Factors involved in the production of liposomes with a high-pressure homogenizer. *International Journal of Pharmaceutics*, *213*, 175–186.

Bryła, A., Lewandowicz, G., & Juzwa, W. (2015). Encapsulation of elderberry extract into phospholipid nanoparticles. *Journal of Food Engineering*, *167*, 189–195.

Bunz, F., Dutriaux, A., Lengauer, C., Waldman, T., Zhou, S., Brown, J. P., … Vogelstein, B. (1998). Requirement for p53 and p21 to sustain G2 arrest after DNA damage. *Science*, *282*, 1497–1501.

Calzolai, L., Gilliland, D., & Rossi, F. (2012). Measuring nanoparticles size distribution in food and consumer products: A review. *Food Additives and Contaminants - Part A Chemistry, Analysis, Control, Exposure and Risk Assessment*, *29*, 1183–1193.

Caputo, F., Arnould, A., Bacia, M., Ling, W. L., Rustique, E., Texier, I., … Couffin, A. C. (2019). Measuring Particle Size Distribution by Asymmetric Flow Field Flow Fractionation: A Powerful Method for the Preclinical Characterization of Lipid-Based Nanoparticles. *Molecular Pharmaceutics*, *16*, 756–767.

Caputo, F., Clogston, J., Calzolai, L., Rösslein, M., & Prina-Mello, A. (2019). Measuring particle size distribution of nanoparticle enabled medicinal products, the joint view of EUNCL and NCI-NCL. A step by step approach combining orthogonal measurements with increasing complexity.

442 *Journal of Controlled Release*, *299*, 31–43.
443 Chaib, S., Tchkonia, T., & Kirkland, J. L. (2022). Cellular senescence and senolytics: the path to the
444 clinic. *Nature Medicine*, *28*, 1556–1568.
445 Chen, X., Zou, L., Liu, W., & McClements, D. J. (2016). Potential of Excipient Emulsions for
446 Improving Quercetin Bioaccessibility and Antioxidant Activity: An *in Vitro* Study. *Journal of*
447 *Agricultural and Food Chemistry*, *64*, 3653–3660.
448 Gibis, M., Ruedt, C., & Weiss, J. (2016). *In vitro* release of grape-seed polyphenols encapsulated
449 from uncoated and chitosan-coated liposomes. *Food Research International*, *88*, 105–113.
450 Gibis, M., Zeeb, B., & Weiss, J. (2014). Formation, characterization, and stability of encapsulated
451 hibiscus extract in multilayered liposomes. *Food Hydrocolloids*, *38*, 28–39.
452 Gioria, S., Caputo, F., Urbán, P., Maguire, C. M., Bremer-Hoffmann, S., Prina-Mello, A., … Mehn,
453 D. (2018). Are existing standard methods suitable for the evaluation of nanomedicines: Some
454 case studies. *Nanomedicine*, *13*, 539–554.
455 Guldiken, B., Gibis, M., Boyacioglu, D., Capanoglu, E., & Weiss, J. (2017). Impact of liposomal
456 encapsulation on degradation of anthocyanins of black carrot extract by adding ascorbic acid.
457 *Food and Function*, *8*, 1085–1093.
458 Gurău, F., Baldoni, S., Prattichizzo, F., Espinosa, E., Amenta, F., Procopio, A. D., … Olivieri, F.
459 (2018). Anti-senescence compounds: A potential nutraceutical approach to healthy aging.
460 *Ageing Research Reviews*, *46*, 14–31.
461 Haddadzadegan, S., Dorkoosh, F., & Bernkop-Schnürch, A. (2022). Oral delivery of therapeutic
462 peptides and proteins: Technology landscape of lipid-based nanocarriers. *Advanced Drug*
463 *Delivery Reviews*, *182*, 114097.
464 Hao, J., Guo, B., Yu, S., Zhang, W., Zhang, D., Wang, J., & Wang, Y. (2017). Encapsulation of the
465 flavonoid quercetin with chitosan-coated nano-liposomes. *LWT*, *85*, 37–44.
466 Hwang, H. T. V., Tran, D. T., Rebuffatti, M. N., Li, C. S., & Knowlton, A. A. (2018). Investigation
467 of quercetin and hyperoside as senolytics in adult human endothelial cells. *PLoS ONE*, *13*, 1–

14.

Iavicoli, P., Urbán, P., Bella, A., Ryadnov, M. G., Rossi, F., & Calzolai, L. (2015). Application of Asymmetric Flow Field-Flow Fractionation hyphenations for liposome-antimicrobial peptide interaction. *Journal of Chromatography A*, *1422*, 260–269.

Ibišević, M., Smajlović, A., & Arsić, I. (2019). Optimization of high pressure homogenization in the production of liposomal dispersions. *Technologica Acta*, *12*, 7–10.

ISO. (2018). ISO - ISO/TS 21362:2018 - Nanotechnologies — Analysis of nano-objects using asymmetrical-flow and centrifugal field-flow fractionation, 38.

ISO. (2019). ISO - ISO 18747-2:2019 - Determination of particle density by sedimentation methods — Part 2: Multi-velocity approach.

Kirkland, J. L., & Tchkonia, T. (2017). Cellular Senescence: A Translational Perspective. *EBioMedicine*, *21*, 21–28.

Li, Y., Le Maux, S., Xiao, H., & McClements, D. J. (2009). Emulsion-based delivery systems for tributyrin, a potential colon cancer preventative agent. *Journal of Agricultural and Food Chemistry*, *57*, 9243–9249.

Liu, W., Hou, Y., Jin, Y., Wang, Y., Xu, X., & Han, J. (2020). Research progress on liposomes: Application in food, digestion behavior and absorption mechanism. *Trends in Food Science and Technology*, *104*, 177–189.

Madureira, A. R., Campos, D. A., Fonte, P., Nunes, S., Reis, F., Gomes, A. M., … Pintado, M. M. (2015). Characterization of solid lipid nanoparticles produced with carnauba wax for rosmarinic acid oral delivery. *RSC Advances*, *5*, 22665–22673.

Malekar, S. A., Sarode, A. L., Bach, A. C., & Worthen, D. R. (2016). The Localization of Phenolic Compounds in Liposomal Bilayers and Their Effects on Surface Characteristics and Colloidal Stability. *AAPS PharmSciTech*, *17*, 1468–1476.

Mária, J., & Ingrid, Ž. (2017). Effects of bioactive compounds on senescence and components of senescence associated secretory phenotypes *in vitro*. *Food and Function*, *8*, 2394–2418.

McClements, D. J. (2018). Delivery by Design (DbD): A Standardized Approach to the Development of Efficacious Nanoparticle- and Microparticle-Based Delivery Systems. *Comprehensive Reviews in Food Science and Food Safety*, *17*, 200–219.

Mehn, D., Capomaccio, R., Gioria, S., Gilliland, D., & Calzolai, L. (2020). Analytical ultracentrifugation for measuring drug distribution of doxorubicin loaded liposomes in human serum. *Journal of Nanoparticle Research*, *22*, 1–7.

Mehn, D., Caputo, F., Rösslein, M., Calzolai, L., Saint-Antonin, F., Courant, T., … Gilliland, D. (2017). Larger or more? Nanoparticle characterisation methods for recognition of dimers. *RSC Advances*, *7*, 27747–27754.

Mehn, D., Iavicoli, P., Cabaleiro, N., Borgos, S. E., Caputo, F., Geiss, O., … Gilliland, D. (2017). Analytical ultracentrifugation for analysis of doxorubicin loaded liposomes. *International Journal of Pharmaceutics*, *523*, 320–326.

Parot, J., Caputo, F., Mehn, D., Hackley, V. A., & Calzolai, L. (2020). Physical characterization of liposomal drug formulations using multi-detector asymmetrical-flow field flow fractionation. *Journal of Controlled Release*, *320*, 495–510.

Planken, K. L., & Cölfen, H. (2010). Analytical ultracentrifugation of colloids. *Nanoscale*, *2*, 1849–1869.

Quach, H., Le, T. V., Nguyen, T. T., Nguyen, P., Nguyen, C. K., & Dang, L. H. (2022). Nano-Lipids Based on Ginger Oil and Lecithin as a Potential Drug Delivery System. *Pharmaceutics*, *14*, 1–15.

Robert, C., Couëdelo, L., Vaysse, C., & Michalski, M. C. (2020). Vegetable lecithins: A review of their compositional diversity, impact on lipid metabolism and potential in cardiometabolic disease prevention. *Biochimie*, *169*, 121–132.

Toniazzo, T., Peres, M. S., Ramos, A. P., & Pinho, S. C. (2017). Encapsulation of quercetin in liposomes by ethanol injection and physicochemical characterization of dispersions and lyophilized vesicles. *Food Bioscience*, *19*, 17–25.

Wagner, A., & Vorauer-Uhl, K. (2011). Liposome Technology for Industrial Purposes. *Journal of Drug Delivery*, *2011*, 1–9.

Zhou, H., & McClements, D. J. (2022). Recent Advances in the Gastrointestinal Fate of Organic and Inorganic Nanoparticles in Foods. *Nanomaterials*, *12*, 1–19.

Figure captions

Figure 1 Size distribution measured with AUC of liposomes (black line) and liposomes with quercetin (dotted black line) calculated from the absorption-based measurement at 250 nm. Grey line indicates the distribution of loaded liposomes with adsorption-based measurement at 370 nm.

Figure 2 MD-AF4 fractograms of liposomes (a) and loaded liposomes with quercetin (b). Black line: UV-Vis linear response at 250 nm; yellow dots: hydrodynamic diameter obtained by DLS in flow mode; green and red dots: geometric diameter of the first two size populations detected by MALS and elaborated by the Zimm model; violet dots: geometric diameter of the third size population detected by MALS and calculated by the Sphere model. The maximum recovery for both loaded and unloaded liposomes is reported in the insight.

Figure 3 cryo-TEM micrographs of liposomes.

Figure 4 Quercetin-loaded liposomes affect cell metabolism in a colon cancer cells model. MTS assay on HCT-116 $p53^{+/+}$ cells. Cells were treated with increasing amounts of free quercetin (free Q), unloaded liposomes (L), or quercetin-loaded liposomes (QL) at the indicated concentrations for 48 h. In graph, the percentage of metabolic activity relative to untreated cells (for L- and QL-treated cells) and to DMSO-treated cells (for free Q-treated cells), both arbitrary set to 100%, is represented. Values are mean ± SD (n=3).

Figure S 1 Particle size distribution as a function of intensity (%) of liposomes (solid line) and liposomes containing quercetin (dotted line) obtained by high-speed homogenizer (a), and HPH at 50 (b), 100 (c), 150 (d) MPa for 1 pass and 150 MPa for 3 passes (e).

Table (Editable version)

Table 1 Absorbance at 660 nm, ζ-potential, Z average (Z-ave), polydispersity index (PDI) and encapsulation efficiency (EE) of liposomes with and without quercetin produced by high-speed homogenization (control) and high-pressure homogenization (HPH) at different conditions.

Presence of quercetin	Homogenization pressure	Number of passes	Turbidity (-)	Z-ave (nm)	PDI (-)	ζ-potential (mV)	EE (%)
without quercetin	0 (control)	-	0.405 ± 0.003 ^{a,B}	163.8 ± 2.4 ^{a,B}	0.522 ± 0.008 ^{a,A}	-20.20 ± 0.79 ^{a,B}	
	50 MPa	1	0.122 ± 0.004 ^{b,B}	96.1 ± 1.5 ^{b,B}	0.349 ± 0.035 ^{b,B}	-21.87 ± 1.11 ^{bc,A}	
	100 MPa	1	0.055 ± 0.001 ^{d,B}	73.4 ± 1.4 ^{c,B}	0.292 ± 0.019 ^{cd,B}	-20.73 ± 0.68 ^{ab,A}	
	150 MPa	1	0.047 ± 0.001 ^{e,B}	69.3 ± 0.8 ^{d,B}	0.282 ± 0.007 ^{d,B}	-23.72 ± 0.62 ^{d,B}	
	150 MPa	3	0.062 ± 0.001 ^{c,A}	53.7 ± 1.5 ^{e,B}	0.331 ± 0.035 ^{bc,B}	-22.08 ± 0.45 ^{c,B}	
with quercetin	0 (control)	-	0.720 ± 0.001 ^{a,A}	267.0 ± 10.2 ^{a,A}	0.529 ± 0.018 ^{a,A}	-18.50 ± 1.21 ^{a,A}	32.93 ± 0.12^{b}
	50 MPa	1	0.282 ± 0.062 ^{b,A}	117.0 ± 4.4 ^{b,A}	0.437 ± 0.027 ^{b,A}	-21.70 ± 1.10 ^{b,A}	37.04 ± 0.13^{ab}
	100 MPa	1	0.109 ± 0.028 ^{c,A}	88.4 ± 6.3 ^{c,A}	0.464 ± 0.049 ^{b,A}	-21.58 ± 1.33 ^{b,A}	34.13 ± 0.24^{b}
	150 MPa	1	0.085 ± 0.001 ^{c,A}	92.6 ± 1.2 ^{c,A}	0.323 ± 0.009 ^{c,A}	-21.94 ± 1.39 ^{b,A}	42.11 ± 4.08^{a}
	150 MPa	3	0.056 ± 0.000 ^{c,B}	72.0 ± 2.9 ^{d,A}	0.550 ± 0.019 ^{a,A}	-20.04 ± 0.81 ^{ab,A}	31.19 ± 0.06^{b}

Mean ± standard deviation (n>2). $^{a-e}$: means indicated a significant difference (p<0.05) among different treatments; $^{A-B}$: means indicated a significant difference (p<0.05) among loaded and unloaded liposomes.

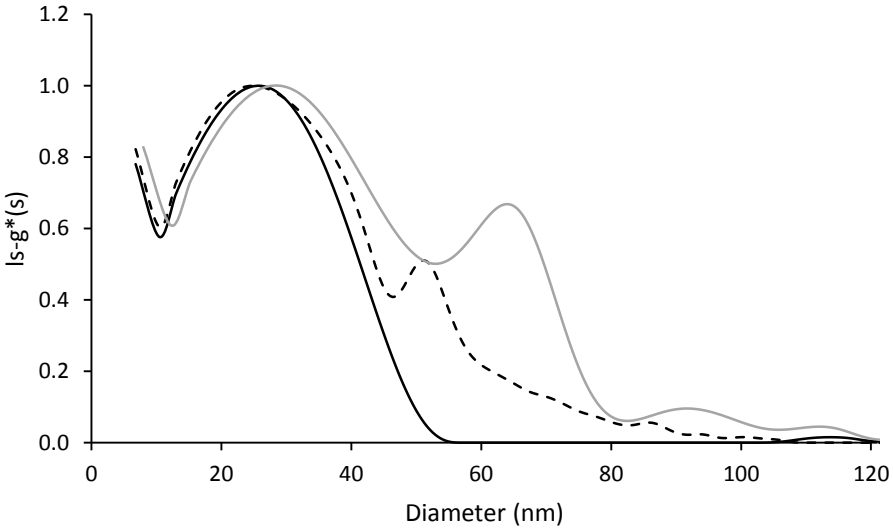

Figure 1

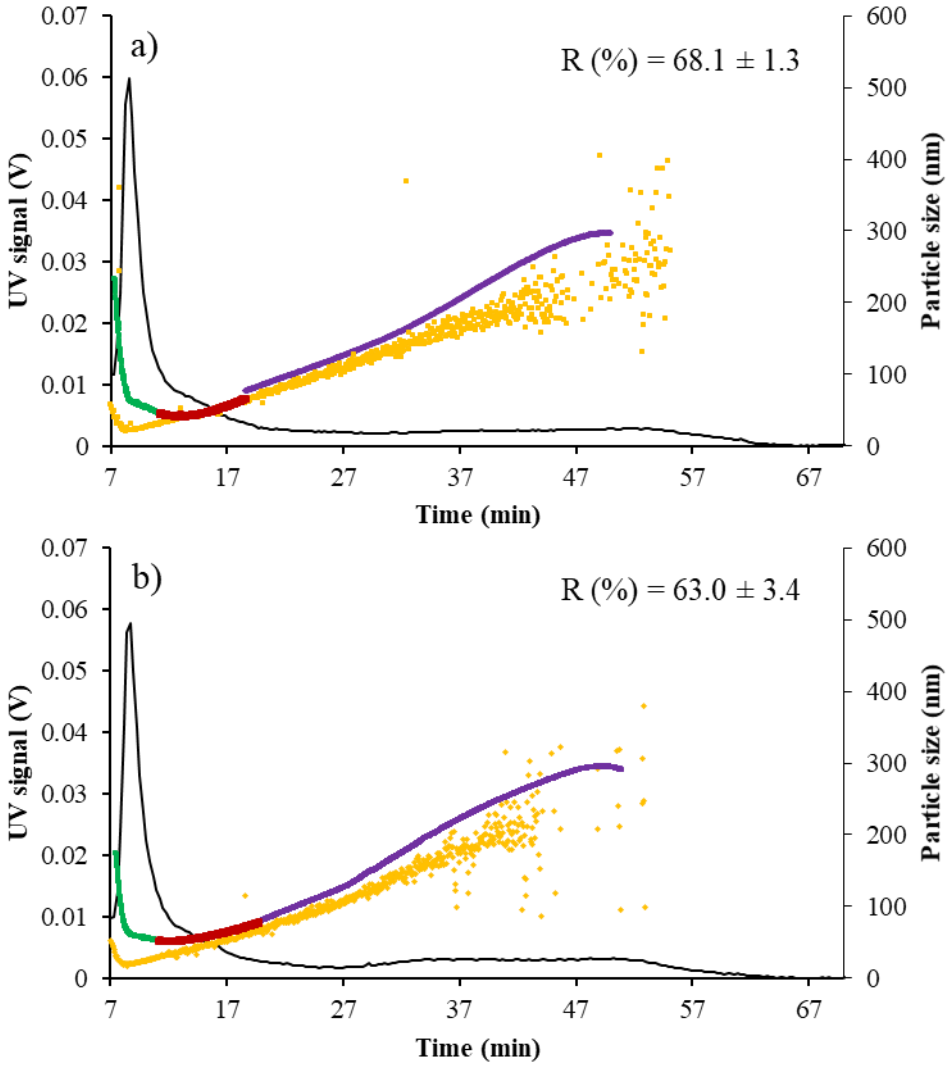

Figure 2

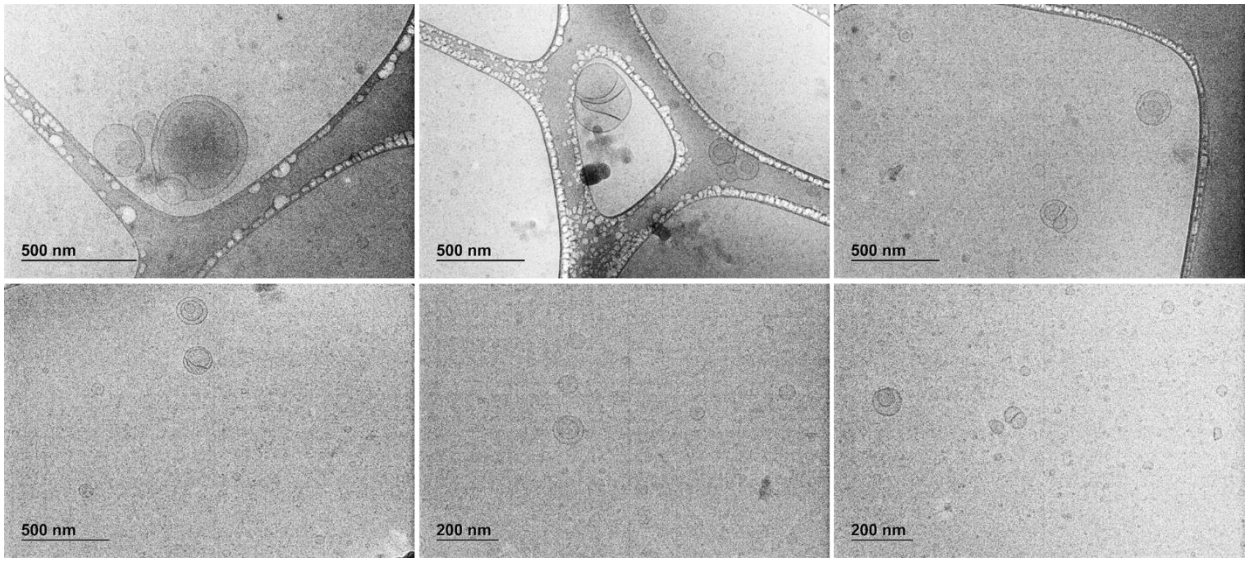

Figure 3

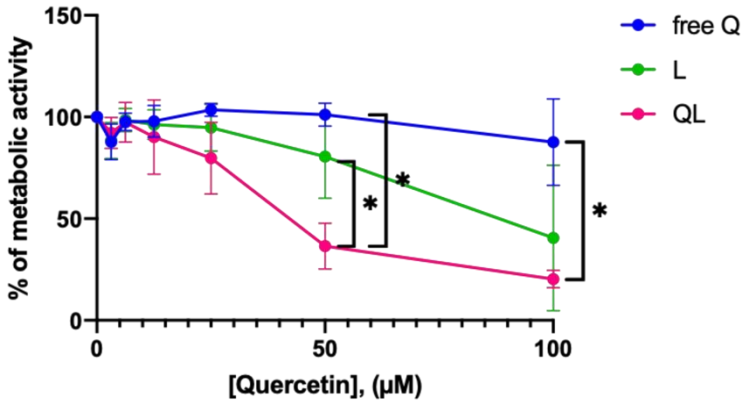

Figure 4

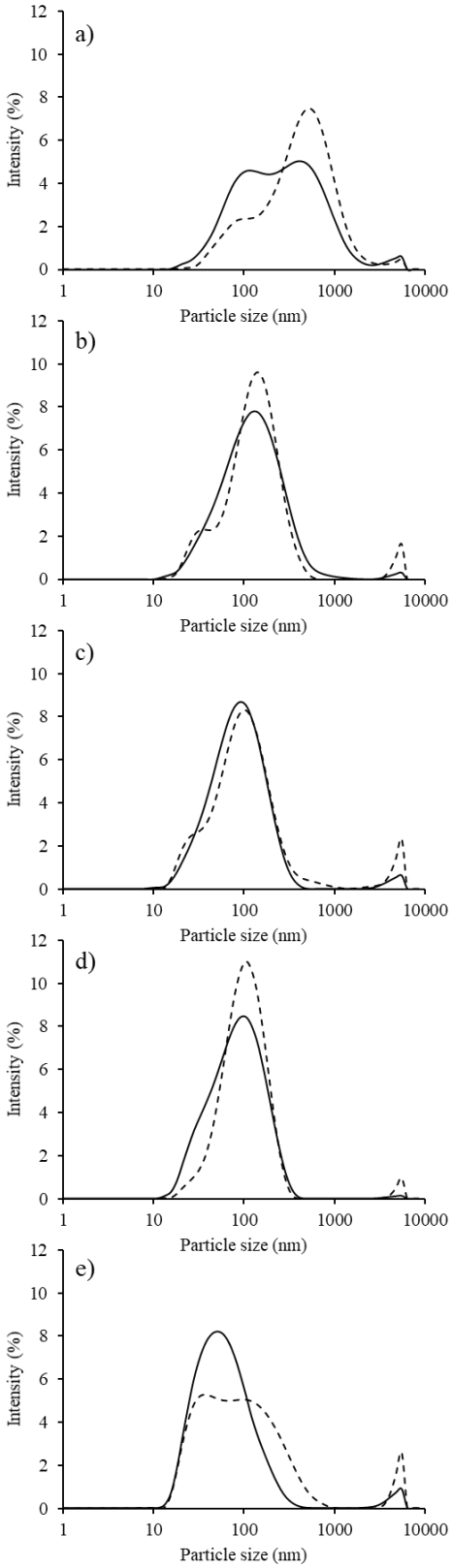

Figure S 1

Graphical Abstract

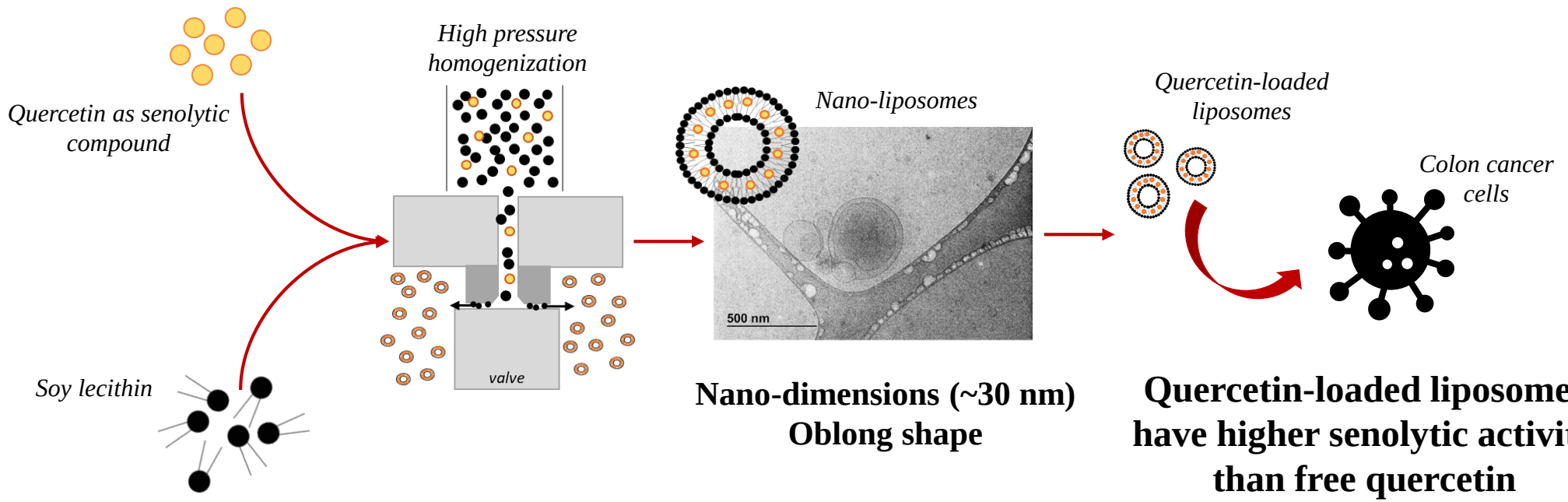

Nano-dimensions (~30 nm)
Oblong shape

Quercetin-loaded liposomes have higher senolytic activity than free quercetin

Author Conflict of Interest Declaration

We wish to confirm that there are no known conflicts of interest associated with this publication and there has been no significant financial support for this work that could have influenced its outcome.

We confirm that the manuscript has been read and approved by all named authors and that there are no other persons who satisfied the criteria for authorship but are not listed. We further confirm that the order of authors listed in the manuscript has been approved by all of us.

We confirm that we have given due consideration to the protection of intellectual property associated with this work and that there are no impediments to publication, including the timing of publication, with respect to intellectual property. In so doing we confirm that we have followed the regulations of our institutions concerning intellectual property.

We further confirm that any aspect of the work covered in this manuscript that has involved experimental animals has been conducted with the ethical approval of all relevant bodies and that such approvals are acknowledged within the manuscript.

We understand that the Corresponding Authors are the sole contact for the Editorial process (including Editorial Manager and direct communications with the office). They are responsible for communicating with the other authors about progress, submissions of revisions and final approval of proofs. We confirm that we have provided a current, correct email address which is accessible by the Corresponding Authors (sofia.melchior@uniud.it and luigi.calzolai@ec.europa.eu).

Udine, 27 February 2023

Signed by the Corresponding Authors on behalf of all authors:

Sofia Melchior

Luigi Calzolai